# Automatic parameter setting for Arnoldi-Tikhonov methods

S. Gazzola, P. Novati
Department of Mathematics
University of Padova, Italy

March 16, 2012

**Abstract**

In the framework of iterative regularization techniques for large-scale linear ill-posed problems, this paper introduces a novel algorithm for the choice of the regularization parameter when performing the Arnoldi-Tikhonov method. Assuming that we can apply the discrepancy principle, this new strategy can work without restrictions on the choice of the regularization matrix. Moreover this method is also employed as a procedure to detect the noise level whenever it is just overestimated. Numerical experiments arising from the discretization of integral equations and image restoration are presented.

## 1 Introduction

In this paper we consider the solution of ill-conditioned linear systems of equations

$$Ax = b, \quad A \in \mathbb{R}^{N\times N}, \quad b \in \mathbb{R}^N, \tag{1}$$

in which the matrix $A$ is assumed to have singular values that rapidly decay and cluster near zero. These kind of systems typically arise from the discretization of linear ill-posed problem, such as Fredholm integral equations of the first kind with a compact kernel; for this reason they are commonly referred to as linear discrete ill-posed problems (see [5], Chapter 1, for a background).

While working with this class of problems, one commonly assumes that the available right-hand side vector $b$ is affected by noise, caused by measurement or discretization errors. Therefore, throughout the paper we suppose that

$$b = \overline{b} + e,$$

where $\overline{b}$ represents the unknown noise-free right-hand side, and we denote by $\overline{x}$ the solution of the error-free system $Ax = \overline{b}$. We also assume that a fairly accurate estimate of $\varepsilon = \|e\|$ is known, where $\|\cdot\|$ denotes the Euclidean norm.

Because of the ill-conditioning of $A$ and the presence of noise in $b$, some sort of regularization is generally employed to find a meaningful approximation of $\overline{x}$. In this framework, a popular and well-established regularization technique is Tikhonov method, which consists in solving the minimization problem

$$\min_{x \in \mathbb{R}^n} \left\{ \|Ax - b\|^2 + \lambda \|Lx\|^2 \right\}, \tag{2}$$

where $\lambda > 0$ is the regularization parameter and $L \in \mathbb{R}^{(N-p)\times N}$ is the regularization matrix (see e.g. [3] and [5], Chapter 5, for a background). We denote the solution of (2) by $x_\lambda$. Common choices for $L$ are the identity matrix $I_N$ (in this case (2) is said to be in standard form) or scaled finite differences approximations of the first or the second order derivative (when $L \neq I_N$ (2) is said to be in general form). We remark that, especially when one has a good intuition of the behavior of the solution $\overline{x}$, a regularization matrix different from the identity can considerably improve the quality of the approximation given by the solution of (2). The ideal situation is when the features of the exact solution that one wants to preserve belong to the null space of the matrix $L$, since $L$ acts as a penalizing filter (see [14] and the references therein for a deeper discussion).

The choice of $\lambda$ is also crucial, since it weights the penalizing term and so specifies the amount of regularization one wants to impose. Many techniques have been developed to determine a suitable value for the regularizing parameter, usually based on the amount of knowledge of the error on $b$ (again we refer to [5], Chapter 7, for an exhaustive background; we also quote the recent paper [15] for the state of the art). When a fairly accurate approximation of $\varepsilon$ is available (as in our case), a widely used method is the so-called discrepancy principle. It prescribes to take, as regularization parameter, the value of $\lambda$ that solves the following equation

$$\|b - Ax_\lambda\| = \eta\varepsilon, \tag{3}$$

where $\eta > 1$ is a user-specified constant, typically very close to 1. The vector $b - Ax_\lambda$ is called discrepancy.

In this paper we solve (2) using an iterative scheme called Arnoldi-Tikhonov (AT) method, first proposed in [2]. This method has proved to be particularly efficient when dealing with large scale problems, as for instance the ones arising from image restoration. Indeed, it is based on the projection of the original problem (2) onto Krylov subspaces of smaller dimensions computed by the Arnoldi algorithm. For reasons closely related to the parameter choice strategy, this method has been experimented mostly when (2) is in standard form [10]. Recently, an extension which employs the generalized Krylov subspaces and that therefore can deal with general form problems, has been introduced in [14].

Here we mainly focus the attention on general form problems, but we adopt a different approach from the one derived in [14], since we work with the usual Krylov subspaces $\mathcal{K}_m(A, b) = \text{span}\{b, Ab, \ldots, A^{m-1}b\}$ (or, if an approximate solution $x_0$ is available, with $\mathcal{K}_m(A, b - Ax_0)$). We call this method Generalized

Arnoldi-Tikhonov (GAT) to avoid confusion with the standard implementation of the AT method. The parameter choice strategy presented in this paper is extremely simple and does not require the problem (2) to be in standard form. Moreover, this new algorithm can handle rectangular matrices $L$, which is an evident advantage since in many applications this option is the most natural one. Our basic idea is to use a linear approximation of the discrepancy

$$\|b - Ax_m\| \approx \alpha_m + \lambda\beta_m,$$

where $x_m$ is the $m$th approximation of the GAT method, and to solve with respect to $\lambda$ the corresponding equation

$$\alpha_m + \lambda\beta_m = \eta\varepsilon.$$

As we shall see, the value of $\alpha_m$ in the above equation will be just the GMRES residual, whereas $\beta_m$ will be defined using the discrepancy of the previous step. In this way, starting from an initial guess $\lambda_0$, we will actually construct a sequence of parameters $\lambda_1, \lambda_2, ...$, such that $\lambda_{m-1}$ will be used to compute $x_m$ until the discrepancy principle (3) is satisfied. We will be able to demonstrate that the the above technique is in fact a secant zero finder.

As we shall see, the procedure is extremely simple and does not require any hypothesis on the regularization matrix $L$. For this reason, in the paper we also consider the possibility of using the GAT method to approximate the noise level $\varepsilon$ whenever it is just overestimated by a quantity $\bar{\varepsilon} > \varepsilon$. In a situation like this the discrepancy principle generally yields poor results if the approximation of $\varepsilon$ is coarse. Anyway, our idea consists in restarting the GAT method, and to use the observed discrepancy to improve the approximation of $\varepsilon$ step by step. The examples so far considered have demonstrated that this approach is really effective, and the additional expense due to the restarts of the GAT method does not heavily affect the total amout of work. This is due to the fact that the GAT method is extremely fast whenever an initial approximation $x_0$ is available.

The paper is organized as follows. In Section 2 we review the AT method and we describe its generalized version, the GAT method. In Section 3 we introduce the new technique for the choice of $\lambda$. In Section 4 we display the results obtained performing common test problems, as well as some examples of image restoration. In Section 5 we suggest an extension of the previous method that allows to work even when the quantity $\varepsilon$ is overestimated. Finally, in Section 6, we propose some concluding remarks.

## 2 The Arnoldi-Tikhonov method

The Arnoldi-Tikhonov (AT) method has been introduced in [2] with the basic aim of reducing the problem

$$\min_{x \in \mathbb{R}^N} \left\{ \|Ax - b\|^2 + \lambda \|Lx\|^2 \right\}, \tag{4}$$

in the case of $L = I_N$, to a problem of much smaller dimension. The idea is to project the matrix $A$ onto the Krylov subspaces generated by $A$ and the vector $b$, i.e., $\mathcal{K}_m(A, b) = \text{span}\{b, Ab, \ldots, A^{m-1}b\}$, with $m \ll N$. The method was even introduced to avoid the matrix-vector multiplication with $A^T$ required by Lanczos type schemes (see e.g [1], [2], [8], [11]). For the construction of the Krylov subspaces the AT method uses the Arnoldi algorithm (see [16], Section 6.3, for an exhaustive background), which yields the decomposition

$$AV_m = V_{m+1}H_{m+1}, \tag{5}$$

where $V_{m+1} = [v_1, ..., v_{m+1}] \in \mathbb{R}^{N\times(m+1)}$ has orthonormal columns which span the Krylov subspace $\mathcal{K}_m(A, b)$ and $v_1$ is defined as $b/\|b\|$. The matrix $H_{m+1} \in \mathbb{R}^{(m+1)\times m}$ is an upper Hessenberg matrix. Denoting by $h_{i,j}$ the entries of $H_{m+1}$, in exact arithmetics the Arnoldi process arrests whenever $h_{m+1,m} = 0$, which means $\mathcal{K}_{m+1}(A, b) = \mathcal{K}_m(A, b)$.

The AT method searches for approximations belonging to $\mathcal{K}_m(A, b)$. In this sense, replacing $x = V_m y_m$ ($y_m \in \mathbb{R}^m$) into (4) with $L = I_N$, yields the following reduced minimization problem

$$\min_{y_m\in\mathbb{R}^m} \left\{ \left\| H_{m+1}y_m - V_{m+1}^T b \right\|^2 + \lambda \|y_m\|^2 \right\}, \tag{6}$$

since $V_m^T V_m = I_m$. Remembering that $v_1 = b/\|b\|$ we also obtain

$$V_{m+1}^T b = \|b\| e_1, \text{ where } e_1 = (1, 0, ..., 0)^T \in \mathbb{R}^{m+1}.$$

Looking at (6), we can say that the AT method can be regarded to as a regularized version of the GMRES. We remark that a variant of this method, the so called Range Restricted Arnoldi-Tikhonov (RRAT) method, has been proposed in [10]. The RRAT method consists in starting the Arnoldi process with $v_1 = Ab/\|Ab\|$, i.e. to work with the Krylov subspaces $\mathcal{K}_m(A, Ab) = \text{span}\{Ab, A^2b, ..., A^mb\}$, which leads again to (6), but with a different $H_{m+1}$ and $V_{m+1}$. The basic aim of this variant, which in general can be applied to many Krylov solver, is to reduce the noise contained in $b$, at the beginning, considering the product $Ab$. For both methods (AT and RRAT) the solution of (4) is then approximated by $x_m = V_m y_m$.

The method considered in this paper is an extension of the AT method in order to work with a general regularization operator $L \neq I_N$ and with an arbitrary starting vector $x_0$. We consider the minimization problem

$$\min_{x\in\mathbb{R}^N} \left\{ \|Ax - b\|^2 + \lambda \|L(x - x_0)\|^2 \right\}, \tag{7}$$

which is a slight modification of (4) that allows to incorporate an initial approximation $x_0$ of the exact solution (eventually, if $x_0$ is not available, we consider $x_0 = 0$ and we definitely solve (4)). We search for approximations of the type

$$x_m = x_0 + V_m y_m, \tag{8}$$

where $V_m \in \mathbb{R}^{N\times m}$ is defined as in (5), except that now its columns form an orthonormal basis of the Krylov subspace $\mathcal{K}_m(A, r_0)$, where $r_0 = b - Ax_0$. Substituting (8) into (7) we obtain the reduced minimization problem

$$\begin{aligned} & \min_{y_m\in\mathbb{R}^m} \left\{ \|AV_m y_m - r_0\|^2 + \lambda \|LV_m y_m\|^2 \right\} \\ = & \min_{y_m\in\mathbb{R}^m} \left\{ \|H_{m+1} y_m - \|r_0\| \, e_1\|^2 + \lambda \|LV_m y_m\|^2 \right\}, \end{aligned}$$

which can be rewritten as the following least square problem

$$\min_{y_m\in\mathbb{R}^m} \left\| \begin{pmatrix} H_{m+1} \\ \sqrt{\lambda} LV_m \end{pmatrix} y_m - \begin{pmatrix} \|r_0\| \, e_1 \\ 0 \end{pmatrix} \right\|^2. \tag{9}$$

In the sequel we will refer to the above reduced minimization problem as Generalized Arnoldi-Tikhonov (GAT) method.

We note that the problem (9) has a coefficient matrix of dimension $[(m+1)+(N-p)]\times m$, since, in general, $L \in \mathbb{R}^{(N-p)\times N}$. At a first glance, this formulation could seem computationally disadvantageous, if compared to (6), where the matrix $LV_m$ is replaced by the identity matrix of order $m$ and the coefficient matrix of the corresponding least square problem has dimension $(2m+1)\times m$. However, we remark that the GAT method can deal with arbitrary regularization matrices so that this drawback is usually balanced by the positive effect that a suitable $L$ can have on noisy problems. Furthermore, it is very important to observe that the GAT method and, in general, each Krylov solver based on the construction of the Krylov subspaces $\mathcal{K}_m(A, b)$, is generally very fast for discrete ill-posed problems, and hence the number of columns of the matrix in (9) is very small; therefore this computational disadvantage is actually negligible, as revealed by many numerical experiments. Of course, with the word "fast" we just mean that the approximations rapidly achieve the best attainable accuracy since for this kind of problems an iterative solver typically exhibits semiconvergence or, at best, stagnates.

# 3 The parameter selection strategy

As already said in the Introduction, we assume to know $\varepsilon = \|b - \bar{b}\|$. Under this hypothesis, it turns out that a successful strategy to define a suitable regularization parameter, as well as a stopping criterium, is the discrepancy principle (3) adapted to the iterative setting of the AT (or GAT) method. At each iteration we can define the function $\phi_m(\lambda) = \|b - Ax_{m,\lambda}\|$ and we say that the discrepancy principle is satisfied as soon as

$$\phi_m(\lambda) \leq \eta\varepsilon,$$

where $\eta \gtrapprox 1$. We remark that if we rather know the norm of the relative amount of noise $\widetilde{\varepsilon} = \|e\|/\|\bar{b}\|$, then the discrepancy principle reads

$$\phi_m(\lambda) = \eta\widetilde{\varepsilon}\|b\|.$$

The quantity $\widetilde{\varepsilon}$ is commonly referred to as noise level.

For the GAT method in which the approximations are of the form $x_{m,\lambda} = x_0 + V_m y_{m,\lambda} \in x_0 + \mathcal{K}_m(A, r_0)$, where $y_{m,\lambda}$ solves (9), the discrepancy can be rewritten as

$$\|b - Ax_{m,\lambda}\| = \|r_0 - AV_m y_{m,\lambda}\| = \|c - H_{m+1} y_{m,\lambda}\|, \tag{10}$$

where $c = V_{m+1}^T r_0 = \|r_0\| e_1 \in \mathbb{R}^{m+1}$. Since $y_{m,\lambda}$ solves the normal equation

$$(H_{m+1}^T H_{m+1} + \lambda V_m^T L^T L V_m) y_{m,\lambda} = H_{m+1}^T c,$$

associated to the least square problem (9), by (10) we obtain

$$\phi_m(\lambda) = \left\| H_{m+1}(H_{m+1}^T H_{m+1} + \lambda V_m^T L^T L V_m)^{-1} H_{m+1}^T c - c \right\|. \tag{11}$$

Dealing with expressions of type (11) for the discrepancy, a standard approach consists in solving, with respect to $\lambda$, the nonlinear equation

$$\phi_m(\lambda) = \eta\varepsilon. \tag{12}$$

In [12] the authors present, for the case $L = I_N$, a cubically convergent zero finder which involves quantities that can be computed quite cheaply. The strategy adopted in [10] is to first determine a suitable value of $m$ (that assures that the equation (12) has a unique solution) and then apply the above mentioned cubic zero finder. However the value of $m$ initially determined may be too small to guarantee a good approximation and usually one or two extra iterations are performed to improve the quality of the solution.

Using the method that we are going to describe, suitable values for $\lambda$ and $m$ are determined simultaneously. Our basic hypothesis is that the discrepancy can be well approximated by

$$\phi_m(\lambda) \approx \alpha_m + \lambda\beta_m, \tag{13}$$

i.e., a linear approximation with respect to $\lambda$, in which $\alpha_m, \beta_m \in \mathbb{R}$ can be easily computed or approximated. For what concerns $\alpha_m$, the Taylor expansion of (11) suggests to chose

$$\alpha_m = \phi_m(0) = \left\| H_{m+1}(H_{m+1}^T H_{m+1})^{-1} H_{m+1}^T c - c \right\|,$$

which is just the norm of the residual of the GMRES, which can be evaluated working in reduced dimension, independently of the choice of $L$. In accordance with our notations, we denote by $y_{m,0}$ the projected GMRES solution, i.e., the solution of

$$\min_{y \in \mathbb{R}^m} \|H_{m+1} y - c\|. \tag{14}$$

For what concerns $\beta_m$, suppose that, at the step $m$, we have used the parameter $\lambda_{m-1}$ (computed at the previous step or, if $m = 1$, given by the user) to

compute $y_{m,\lambda_{m-1}}$, by solving (9) with $\lambda = \lambda_{m-1}$. Then we can easily compute the corresponding discrepancy by (10)

$$\phi_m(\lambda_{m-1}) = \left\| c - H_{m+1} y_{m,\lambda_{m-1}} \right\|, \tag{15}$$

and consequently, using the approximation (13), we obtain

$$\beta_m \approx \frac{\phi_m(\lambda_{m-1}) - \alpha_m}{\lambda_{m-1}}. \tag{16}$$

To select $\lambda_m$ for the next step of the Arnoldi algorithm we impose

$$\phi_{m+1}(\lambda_m) = \eta\varepsilon, \tag{17}$$

and force the approximation

$$\phi_{m+1}(\lambda_m) \approx \alpha_m + \lambda_m \beta_m. \tag{18}$$

Hence by, (16) and (17), we define

$$\lambda_m = \frac{\eta\varepsilon - \alpha_m}{\phi_m(\lambda_{m-1}) - \alpha_m} \lambda_{m-1}. \tag{19}$$

The method (19) has a simple geometric interpretation which allows to see it as a zero finder. Indeed, we know that $\phi_m(\lambda)$ is a monotonically increasing function such that $\phi_m(0) = \alpha_m$ (cf. also [10]). Hence, the linear function

$$f(\lambda) = \alpha_m + \lambda \left( \frac{\phi_m(\lambda_{m-1}) - \alpha_m}{\lambda_{m-1}} \right),$$

interpolates $\phi_m(\lambda)$ at 0 and $\lambda_{m-1}$, and the new parameter $\lambda_m$ is obtained by solving $f(\lambda) = \eta\varepsilon$. Hence (19) is just a secant method in which the leftmost point is $(0, \alpha_m)$. In the very first steps of (19) instability can occur: this is due to the fact that we may have $\alpha_m > \eta\varepsilon$. In this situation the result of (19) may be negative and therefore we use

$$\lambda_m = \left| \frac{\eta\varepsilon - \alpha_m}{\phi_m(\lambda_{m-1}) - \alpha_m} \right| \lambda_{m-1}. \tag{20}$$

Anyway, we know that, independently of the definition of $\lambda_{m-1}$, after some steps $\alpha_m < \eta\varepsilon$ (compare also the arguments given in [10]) so that (20) actually represents one step of a zero finder. In Figure 1 we display what typically happens at the $m$-th iteration of the GAT method when the condition $\alpha_m < \eta\varepsilon$ is satisfied.

Numerically, formula (20) is very stable, in the sense that after the discrepancy principle is satisfied, $\lambda_m \approx const.$ This is due to the fact that both $\phi_m(\lambda_{m-1})$ and $\alpha_m = \phi_m(0)$ stagnates. Indeed, since the approximations are computed minimizing the residual within a Krylov subspace, whenever $\mathcal{K}_{m+1}(A, b) \approx \mathcal{K}_m(A, b)$, the values of $\phi_m(\lambda_{m-1})$ and $\alpha_m = \phi_m(0)$ tends to remain almost constant because, in any case $b - AV_m y_{m,\lambda} \in \mathcal{K}_{m+1}(A, b)$, even if the solutions of (9), $y_{m,\lambda_{m-1}}$, and the one of GMRES, $y_{m,0}$, are badly computed.

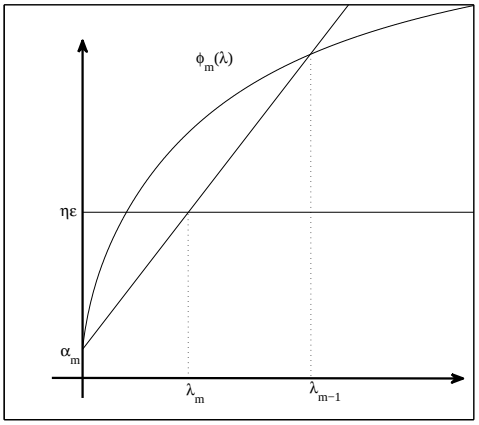


Figure 1: Zero finder interpretation of formula (19).

**Remark 1** *It is interesting to observe that formula (19) is somehow related to the standard techniques used for approximating the local error of a discrete method for ordinary differential equations, whenever a stepsize selection strategy is adopted. Indeed, for a method of order p, the local error at the instant $t_m$ in the interval of integration is of the type*

$$LE_m = c_m h_m^{p+1},$$

*where $c_m$ is an unknown constant depending on the method and the problem, and $h_m$ is the stepsize previously selected. Since an approximation of $LE_m$ is generally known, i.e., $LE_m \approx LE_m^*$, we have*

$$c_m \approx \frac{LE_m^*}{h_m^{p+1}}.$$

*In this way, to define the new stepsize $h_{m+1}$, one imposes*

$$LE_{m+1} = c_{m+1} h_{m+1}^{p+1} \leq \epsilon,$$

*where $\epsilon$ is the prescribed tolerance; forcing $c_{m+1} = c_m$ yields the method*

$$h_{m+1} = \left(\frac{\epsilon}{LE_m^*}\right)^{\frac{1}{p+1}} h_m.$$

*In (19) the role of $LE_m$ and $c_m$ is played by $\phi_m(\lambda_{m-1})$ and $\beta_m$ respectively.*

While not considered in this paper, we remark that this parameter choice technique can also be used together with the Range-Restricted approach [10] and even in the case of Krylov methods based on the Lanczos unsymmetric

process [2]. As already mentioned in the previous sections we again emphasize the fact that the method just described can work without hypothesis on the regularization matrix $L$, and that essentially involves quantities that are strictly connected to the projected problem. At each iteration we simply have to monitor the value of $\phi_m(\lambda)$ for $\lambda = 0$ and $\lambda = \lambda_{m-1}$, so that the only additional cost is due to the computation (in reduced dimension) of the GMRES residual, attainable in $O(m^2)$ operations (if the QR update is not employed, otherwise in just $O(m)$ operations).

If compared to the other parameter choice strategies so far used in connection with the AT method, we realize that the present one is intrinsically simpler and cheaper. In fact, if at each iteration we want to apply the L-curve criterium to the standard form reduced problem (6), as proposed in [2] where this algorithm is referred to as $L_m$-curve method, we have to compute the SVD of $H_{m+1}$ in order to solve the system (9) for many values of $\lambda$. Then we need to employ a reliable algorithm to choose the point of maximum curvature, that sometimes may even provide an unsatisfactory value for $\lambda$. On the other side, using the method proposed in [10], once determined a suitable $m$, we have to apply a convergent zero-finder to solve the nonlinear equation (12). The latter requires, at each step, the value of the first and the second derivative of $\phi_m$ computed for the $\lambda$ determined at the previous step and to do this we have to solve two linear systems of dimension $m$. Actually, since in both cases all the extra computations involve the reduced matrices, we also stress that the computational overload can still be considered negligible. However, the generalization of these strategies to the case of the GAT method is not straightforward: we believe that the most accessible approach is to first transform the problem (4) into standard form (by employing, e.g., the $A$-weighted pseudoinverse of $L$) and then apply the AT method to the transformed problem. Anyway this approach is not as general as the GAT method since, in order to obtain a square matrix associated to the transformed problem, $L$ must be square itself (as explained in [13]). Moreover, this initial transformation affects the overall computational cost because the operations are of course in full-dimension.

Below we present the algorithm used to implement the method.

**Algorithm 2** *Generalized Arnoldi-Tikhonov*
*Input: $A$, $b$, $L$, $x_0$, $\lambda_0$, $\varepsilon$, $\eta$*
*For $m = 1, 2, \ldots$ until $\|b - Ax_{m,\lambda}\| \leq \eta\varepsilon$*

1. *Update $V_m$, $H_{m+1}$ with the Arnoldi algorithm (5);*
2. *Solve (9) with $\lambda = \lambda_{m-1}$ and evaluate $\phi_m(\lambda_{m-1})$ by (15);*
3. *Compute the GMRES solution and evaluate $\alpha_m = \phi_m(0)$;*
4. *Compute the new parameter $\lambda_m$ by (20).*

# 4 Computed examples

To support the new method (20), that from now on we call *secant update*, we show some numerical experiments. In particular, when possible, we compare the performance of our formula with respect to the ones proposed in [2] and [10]. In all the examples we suppose to know the exact solution $\overline{x}$ and the exact right-hand side vector is constructed taking $\overline{b} = A\overline{x}$. The elements of the noise vector $e$ are normally distributed with zero mean and the standard deviation is chosen such that $\|e\|/\|\overline{b}\|$ is equal to a prescribed level $\widetilde{\varepsilon}$. In this section we always take the initial guess $x_0 = 0$ and set $\eta = 1.001$. All the computations have been executed using Matlab 7.10 with 16 significant digits on a single processor computer Intel Core i3-350M.

**Example 1.** We consider a problem coming from a first-kind Fredholm integral equation used to model a one-dimensional image restoration process

$$\int_{-\pi/2}^{\pi/2} K(s,t)f(t)dt \;=\; g(s), \quad -\pi/2 \le s \le \pi/2, \tag{21}$$

where

$$\begin{aligned} K(s,t) &= (\cos(s)+\cos(t))^2 \left(\frac{\sin(u)}{u}\right)^2, \quad u = \pi(\sin(s)+\sin(t)), \\ f(t) &= 2\exp(-6(t-0.8)^2) + \exp(-2(t+0.5)^2). \end{aligned}$$

We use the Matlab code `shaw.m` from [4] in order to discretize (21) using 200 collocation points defined by $t_i = (i-0.5)\pi/200$, $i = 1, \ldots, 200$ and to produce a symmetric matrix $A \in \mathbb{R}^{200\times 200}$ and the solution $\overline{x}$. The condition number of $A$ is around $10^{20}$. We will consider a noise level $\widetilde{\varepsilon} = 10^{-3}$.

In order to present a straightforward comparison with the methods commonly used in connection with the AT method, in this first example we will take $L = I_{200}$. In this context, when we employ the $L_m$-curve criterium, we stop at iteration $\widetilde{m}$ if the norm of the discrepancy associated to the parameter computed using the $L_{\widetilde{m}}$-curve is below the known threshold $\eta\varepsilon$.

In Figure 2 we display the results obtained performing 30 tests (for each test we defined a new perturbed right-hand side to lessen the dependence of the results on the random components of $e$). Both the $L_m$-curve and the secant update method determine a regularized solution which always belongs to the Krylov space $\mathcal{K}_8(A,b)$. However the new method is in every situation the more stable one, since the relative error norms and the values of $\lambda$ determined during the last iteration are always comparable. The same does not hold for the $L_m$-curve method, that on average produces approximated solutions of slightly worse quality. We also show the norms of the relative error and the values of the regularization parameter determined solving the nonlinear equation $\phi_8(\lambda) = \eta\varepsilon$ by Newton's method.

In Figure 3 we plot the solution, corresponding to the test #8 reported in Figure 2, computed using the $L_m$-curve criterium and our secant approach. We

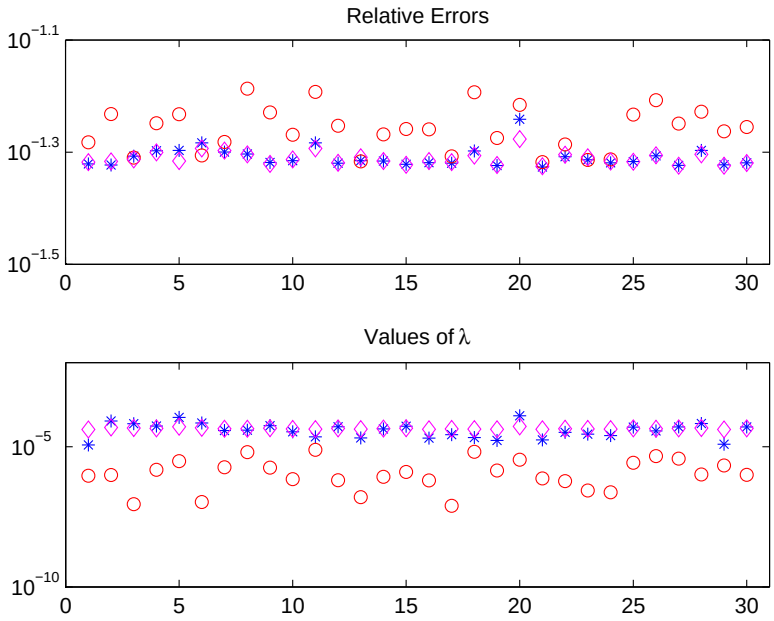


Figure 2: The norms of the relative error (above) and the values of $\lambda$ at the corresponding to the last iteration (below) for each one of the 30 tests performed. The asterisk denotes the secant update method, the circle denotes the $L_m$-curve method and the diamond denotes the values obtained solving $\phi_8(\lambda) = \eta\varepsilon$.

can see that, employing Tikhonov regularization method in standard form, the quality of the solution obtained using both methods are comparable, but the one computed by the $L_m$-curve method shows instability around the solution. This is due to the fact that this criterium allows a slight undersmoothing since it typically selects values of $\lambda$ smaller than the secant update method (cf. Figure 2).

In Figure 4 we compare the behavior of the $L_m$-curve method and the one of our secant update at each iteration. The results correspond to the test #22 reported in Figure 2. Since, in this example, the discrepancy principle is satisfied after only 8 iterations, we decide to compute some extra iterations to evaluate the behavior of both methods after the stopping criterium is fulfilled. In particular, we can note that the secant approach exhibits a very stable progress since, once the threshold is reached, the norm of the discrepancy stagnates and the values of the regularization parameter $\lambda$ remain almost constant.

In Figure 5 we display the values of the regularization parameter, at each iteration, obtained varying the initial value $\lambda_0$ given in input. We choose $\lambda_0 = 0.1, 0.5, 1, 10, 50$. It is quite evident that the strategy is able to de-

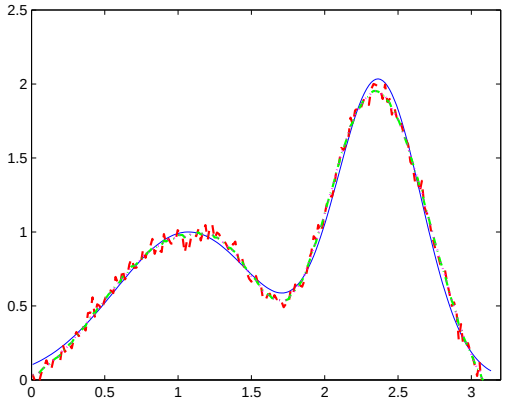


Figure 3: Computed solutions of Example 1. Exact solution (solid line), regularized with the secant update (dash-dot line), regularized with the $L_m$-curve method (dashed line).

termine a suitable value of $\lambda$ independently of the choice of the initial guess. As already said, at the beginning we just force $\lambda_m$ to be positive by (20), and then everything is handled by the condition $\alpha_m < \eta\varepsilon$. Whenever this condition is satisfied, (20) is just a zero finder, so that the curves of $\lambda$ overlap after some steps.

**Example 2.** We now consider some examples coming from 2D image restoration problems. In particular we will focus on the deblurring and denoising of grayscale images, which consists in recovering the $n \times n$ original image $X$ from an available blurred and noisy one $B$ (see [7] for a background). To describe these problems we will obviously adopt a linear model and therefore we write the unknown exact image as $\overline{x} = \text{vect}(X) \in \mathbb{R}^N$, $N = n^2$. We will always consider a Gaussian Point-Spread Function (PSF) defined by

$$h_\sigma(x, y) = \frac{1}{2\pi\sigma^2} \exp\left(-\frac{x^2 + y^2}{2\sigma^2}\right),$$

and zero boundary conditions. This lead to a symmetric Toeplitz matrix given by

$$A = (2\pi\sigma^2)^{-1} T \otimes T \in \mathbb{R}^{N \times N},$$

where $T \in \mathbb{R}^{n \times n}$ is a symmetric banded Toeplitz matrix whose first row is a vector $v$ defined by

$$v_j = \begin{cases} e^{-\frac{(j-1)^2}{2\sigma^2}} & \text{for} \quad j = 1, \ldots, q, \\ 0 & \text{for} \quad j = q+1, \ldots, n. \end{cases}$$

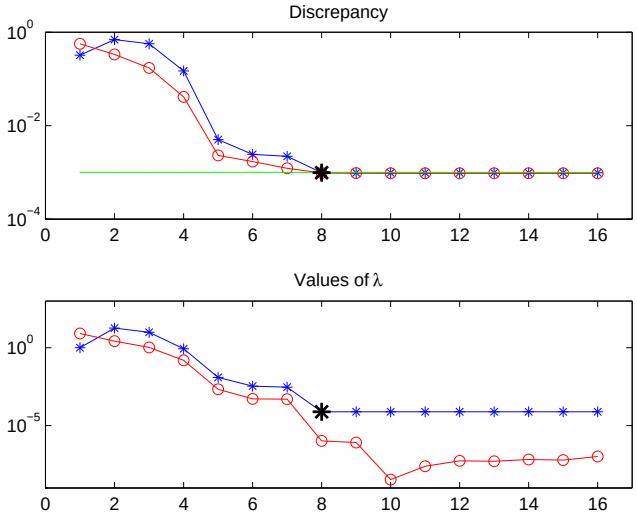


Figure 4: Comparison between the values of the norm of the discrepancy and the values of the regularization parameter computed, at each iteration, by the $L_m$-curve method (circles) and by the secant update (asterisks). The horizontal line in the upper graphic represents the threshold $\eta\varepsilon$. The values corresponding to the 8th iteration, the one at which both methods would stop, are marked with a ticker asterisk.

The parameter $q$ is the half-bandwidth of the matrix $T$, and the parameter $\sigma$ controls the shape of the PSF (the larger $\sigma$, the wider the function). The boundary conditions are set to zero. We use Hansen's function `blur.m` from [6] to build the blurring matrix $A$. We consider a noise level $\widetilde{\varepsilon} = 10^{-2}$ and, as stated at the beginning of this section, we construct the corrupted image, in vector form, as $b = A\overline{x} + e$.

In this context, we will exclusively consider Tikhonov regularization in general form. In the following we list the main regularization matrices that we have employed. We display the matrices in rectangular form and we use the notation $\hat{L}$ when we consider their square versions obtained by appending or prepending a suitable number of rows in such a way that the bidiagonal or tridiagonal

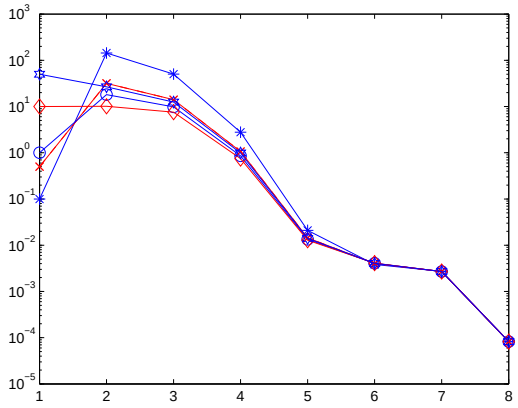


Figure 5: The value of the regularization parameter computed at each iteration by the secant update method, varying the initial guess $\lambda_0$.

pattern of the original matrix is preserved.

$$L_1 \;:=\; \begin{pmatrix} 1 & -1 & & \\ & \ddots & \ddots & \\ & & 1 & -1 \end{pmatrix} \in \mathbb{R}^{(N-1)\times N}, \tag{22}$$

$$L_{1L} \;:=\; \begin{pmatrix} I_n \otimes L_1 \\ L_1 \otimes I_n \end{pmatrix} \in \mathbb{R}^{2n(n-1)\times N}, \tag{23}$$

$$L_{1M} \;:=\; I_n \otimes \hat{L}_1 + \hat{L}_1 \otimes I_n \in \mathbb{R}^{N\times N}, \tag{24}$$

$$L_2 \;:=\; \begin{pmatrix} 1 & -2 & 1 & & \\ & \ddots & \ddots & \ddots & \\ & & 1 & -2 & 1 \end{pmatrix} \in \mathbb{R}^{(N-2)\times N}, \tag{25}$$

$$L_{2L} \;:=\; I_n \otimes \hat{L}_2 + \hat{L}_2 \otimes I_n \in \mathbb{R}^{N\times N}. \tag{26}$$

The operators (22) and (25) represent scaled finite difference approximations of the first and the second derivative, respectively; sometimes The operator (23) is taken from [9], the matrix (26) represents a discretization of the two dimensional Laplace operator. We also introduce the matrix (24) that is the sum of the discretized first derivatives in the vertical and horizontal direction.

Our first task is to compare the performance of the $L_m$-curve criterium and of the new method. We consider the popular test image `peppers.png`, in its original size $256 \times 256$ pixels. The corresponding linear system has dimension 65536. We corrupt the original image using a Gaussian blur whose parameter is $\sigma = 2.5$; we set $q = 6$, $\widetilde{\varepsilon} = 10^{-2}$ and we take $L_2$ as regularization matrix. In order to employ Hansen's function `l_curve.m` from [4] we have slightly modified the

function `cgsvd.m`, belonging to the same package, with the purpose of working with the matrix $L_2V_k$ which has more rows than columns. In Figure 6 we can examine the quality of the reconstruction obtained using both the $L_m$-curve criterium (box (c)) and the secant approach (box (d)). In Figure 7 we report the history of the norm of the relative error and of the discrepancy for both methods. We can see that the restored images are almost identical, even if the norm of the relative error is equal to $7.88 \cdot 10^{-2}$ if we use the $L_m$-curve method and $8.34 \cdot 10^{-2}$ if we use our secant approach; the number of iterations is 9 in the first case, 8 in the second case. However, considering the running time, the difference between the two approaches is more pronounced: using the $L_m$-curve criterium we need 3.05 seconds to compute the solution, while the new method restores the available image in 0.49 seconds. This gap is mainly due to the fact that, using the $L_m$-curve method, at each step we have to evaluate the Generalized Singular Value Decomposition (GSVD) of the matrix pair $(H_{k+1}, L_2V_k)$ and the dimension of second matrix is the same of the unreduced problem.

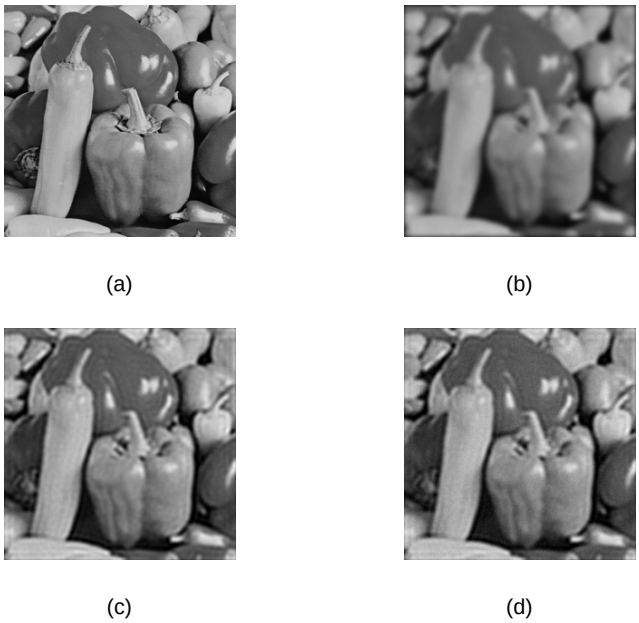


Figure 6: Original image `peppers.png` **(a),** blurred and noisy image **(b)**, restored image with the $L_m$-curve criterium **(c)** and restored image with the secant update method **(d)**.

We now focus exclusively on our method. We want to test the behavior of the GAT method varying the regularization matrix. As a matter of fact the corrupted image is always restored in less than a second and the results obtained

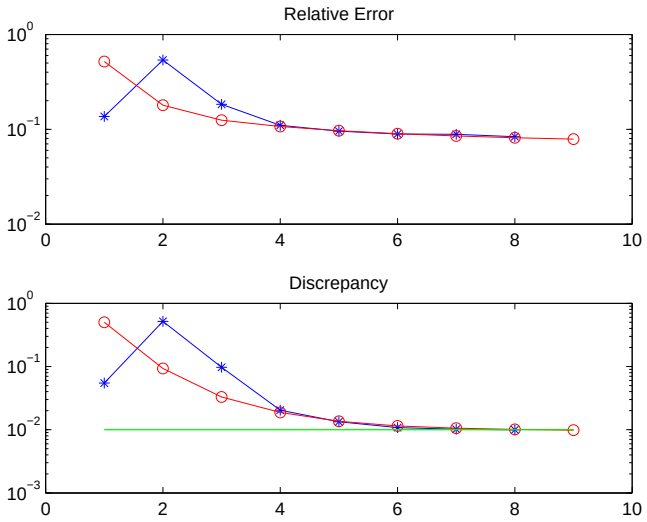


Figure 7: Restoration of `peppers.png`. Comparison between the norm of the relative error (above) and the norm of the discrepancy (below) obtained using the $L_m$-curve criterium (circles) and the secant update (asterisks). The horizontal continuous line marks the threshold $\eta\varepsilon$.

using different regularization matrices taken from the list (22)-(26) are very similar. In particular, since the test image is smooth and lacks of highly definite edges, the best result is obtained applying the second derivative operator $L_2$. To improve the quality of the restoration, once the stopping criterium is fulfilled at a certain step with $\lambda$ as regularization parameter, we try to carry on some extra iterations with $\lambda$ fixed. We will denote this approach with the abbreviation $L_{t,ex}$, where $t$ is one of the subscripts presented in (22)-(26) and $ex$ denotes the number of extra iterations performed.

In Table 1 we record the results obtained considering an underlying Gaussian blur function with $\sigma = 1.5$. The results displayed in Table 2 are relative to $\sigma = 2.5$. The parameter $q$ is set equal to 6 and the noise level $\widetilde{\varepsilon}$ is equal to $10^{-2}$ in both cases.

Finally we consider the performance of the new method applied to the restoration of corrupted medical images. We take the test image `mri.tif` from Matlab, of size $128 \times 128$ pixels, which represents a magnetic resonance image of a section of the human brain. Contrary to the previous test image, the present one is characterized by well marked edges. We again consider a Gaussian blur with parameter $\sigma = 1.5$. The half-bandwidth of $T$ is $q = 6$ and the noise level is equal to $10^{-2}$. In Table 3 we report the results obtained changing the regularization operators and in Figure 8 we show the restored image obtained

| Reg. Matr. | Relative Error | Iterations | Running time (sec) |
|---|---|---|---|
| $I_N$ | $7.3930 \cdot 10^{-2}$ | 4 | 0.21 |
| $L_1$ | $5.5585 \cdot 10^{-2}$ | 6 | 0.34 |
| $L_{1L}$ | $5.5594 \cdot 10^{-2}$ | 6 | 0.39 |
| $L_{1M}$ | $5.5665 \cdot 10^{-2}$ | 6 | 0.31 |
| $L_{1M,4}$ | $5.0402 \cdot 10^{-2}$ | 10 | 0.62 |
| $L_2$ | $5.2268 \cdot 10^{-2}$ | 7 | 0.39 |
| $L_{2L}$ | $5.2423 \cdot 10^{-2}$ | 7 | 0.40 |
| $L_{2L,4}$ | $5.0298 \cdot 10^{-2}$ | 11 | 0.79 |

Table 1: Results of the restoration of `peppers.png` affected by a Gaussian blur with $\sigma = 1.5$ and a noise level equal to $10^{-2}$. In the first column we list the regularization matrices considered.

| Reg. Matr. | Relative Error | Iterations | Running time (sec) |
|---|---|---|---|
| $I_N$ | $1.1268 \cdot 10^{-1}$ | 6 | 0.23 |
| $L_1$ | $8.4488 \cdot 10^{-2}$ | 8 | 0.48 |
| $L_{1L}$ | $8.4487 \cdot 10^{-2}$ | 8 | 0.53 |
| $L_{1M}$ | $8.4446 \cdot 10^{-2}$ | 8 | 0.47 |
| $L_{1M,3}$ | $7.6920 \cdot 10^{-2}$ | 11 | 0.73 |
| $L_2$ | $8.3142 \cdot 10^{-2}$ | 8 | 0.47 |
| $L_{2L}$ | $8.3742 \cdot 10^{-2}$ | 8 | 0.47 |
| $L_{2L,3}$ | $7.6927 \cdot 10^{-2}$ | 11 | 0.80 |

Table 2: Results of the restoration of `peppers.png` affected by a Gaussian blur with $\sigma = 2.5$ and a noise level equal to $10^{-2}$. In the first column we list the regularization matrices considered.

employing the regularization matrix $L_{1M}$ and running the GAT algorithm for 5 extra iterations.

# 5 Noise level detection

The Generalized Arnoldi-Tikhonov method used in connection with the parameter selection strategy presented in Section 3 can be successfully employed also to estimate the noise level $\varepsilon / \left\|\bar{b}\right\|$ if it is not a-priori known. In a situation like this, the discrepancy principle may yield poor results and other techniques such as the L-curve criterium or the GCV method are generally used (here we again quote [15] for a recent overview about the existing parameter choice strategies).

If we assume that that $\varepsilon$ is overestimated by a quantity $\overline{\varepsilon}$, we may expect that applying the GAT method we can fully satisfy the discrepancy principle

| Reg. Matr. | Relative Error | Iterations | Running time (sec) |
|---|---|---|---|
| $I_N$ | $1.8615 \cdot 10^{-1}$ | 6 | 0.07 |
| $L_1$ | $1.8459 \cdot 10^{-1}$ | 6 | 0.10 |
| $L_{1L}$ | $1.8471 \cdot 10^{-1}$ | 6 | 0.10 |
| $L_{1M}$ | $1.8434 \cdot 10^{-1}$ | 6 | 0.08 |
| $L_{1M,5}$ | $1.7078 \cdot 10^{-1}$ | 11 | 0.17 |
| $L_2$ | $1.7704 \cdot 10^{-1}$ | 8 | 0.11 |
| $L_{2L}$ | $1.7700 \cdot 10^{-1}$ | 8 | 0.11 |
| $L_{2L,5}$ | $1.6854 \cdot 10^{-1}$ | 13 | 0.27 |

Table 3: Results of the restoration of `mri.tif` affected by a Gaussian blur with $\sigma = 1.5$ and a noise level equal to $10^{-2}$.

even taking $\eta = 1$, that is,

$$\phi_m(\lambda_{m-1}) < \overline{\varepsilon}, \tag{27}$$

for a given $m$. Applying the secant update method (20) for the definition of the parameter $\lambda$, the discrepancy would then stabilize around $\overline{\varepsilon}$, if the method is not arrested (cf. Figure 4). Our idea is to restart it immediately after (27) is fulfilled, working with the Krylov subspaces generated by $A$ and $b - Ax_{m,\lambda_{m-1}}$, where $x_{m,\lambda_{m-1}}$ is the last approximation obtained. At the same time we define $\overline{\varepsilon} := \phi_m(\lambda_{m-1})$ as the new approximation of the noise. We proceed until the discrepancy is almost constant and we introduce a threshold parameter $\delta$ to check this situation step-by-step. This idea has been implemented following the algorithm given below.

**Algorithm 3** *Restarted Generalized Arnoldi-Tikhonov*
*Input: $A$, $b$, $L$, $\lambda^{(0)}$, $\eta$, $\delta$, and $\varepsilon_0 = \overline{\varepsilon} > \varepsilon$. Define $x^{(0)} = 0$.*
*For $k = 1, 2, \ldots$ until*

$$\frac{\|\varepsilon_k - \varepsilon_{k-1}\|}{\|\varepsilon_{k-1}\|} \leq \delta. \tag{28}$$

1. *Run Algorithm 2 with $x_0 = x^{(k-1)}$, $\varepsilon = \varepsilon_{k-1}$, $\lambda_0 = \lambda^{(k-1)}$. Let $x^{(k)}$ be the last approximation achieved, $\phi^{(k)}$ the corresponding discrepancy norm, and $\lambda^{(k)}$ the last parameter value;*
2. *Define $\varepsilon_k := \phi^{(k)}$;*
3. *Define $\lambda^{(k)} = \frac{\phi^{(k)}}{\phi^{(k-1)}} \lambda^{(k)}$.*

We remark that Step 3 of the above algorithm is rather heuristic. Indeed, Algorithm 2 does not provide a further update for $\lambda$ whenever the discrepancy principle is satisfied, since it is assumed to remain almost constant (cf. Figure 4 and 7). Anyway, in this situation, we may expect that improving the quality of the noise estimate, we have $\phi^{(k)} \leq \phi^{(k-1)}$, so that the corresponding estimated optimal value for $\lambda$ should decrease accordingly, and this is exactly what happens

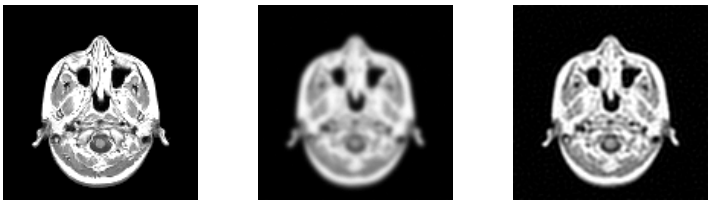

(A) (B) (C)

Figure 8: Restoration of `mri.tif` using $L_{1M,5}$. Original image **(A)**, blurred and noisy image **(B)**, restored image **(C)**.

in practice. The definition in Step 3 ensures that $\lambda^{(k)} \approx const$ whenever $\phi^{(k)} \approx \phi^{(k-1)}$ (cf. (20)).

We test the procedure just described, with and without Step 3 of Algorithm 3, considering again the test image `mri.tif` and, as before, we build the blurring matrix $A$ with parameters $\sigma = 1.5$ and $q = 6$. Then we corrupt the blurred image in order to obtain $\varepsilon / \|b\| = 10^{-3}$. At this point we assume to know only an overestimate $\overline{\varepsilon}$, such that $\overline{\varepsilon} / \|b\| = 10^{-2}$. We employ the regularization matrix $L_{1M}$ defined by (24). In Figure 9 we display the results. We can clearly observe that, after 4 iterations, that is, after the first call of the GAT method, the norm of the discrepancy lays below the overestimated threshold $\overline{\varepsilon}$ At this point we allow the GAT method to restart immediately and to go on until the approximation is satisfactory. The implementation with $\delta = 0.01$, including the last line of Algorithm 3, fulfils the condition (28) after 24 restarts with an estimate $\varepsilon_{24} / \|b\| = 1.03 \cdot 10^{-3}$, while the version without it needs 56 restarts to deliver the estimate $\varepsilon_{56} / \|b\| = 1.05 \cdot 10^{-3}$; in the first case the total running time is 0.48 seconds, in the second case the total running time is 1.45 seconds. In this example, after the first call, the discrepancy principle is always satisfied after the first iteration. If we do not include the update described at Step 3, the

value of $\lambda$ considered at each restart is equal to the one computed at the end of the first call.

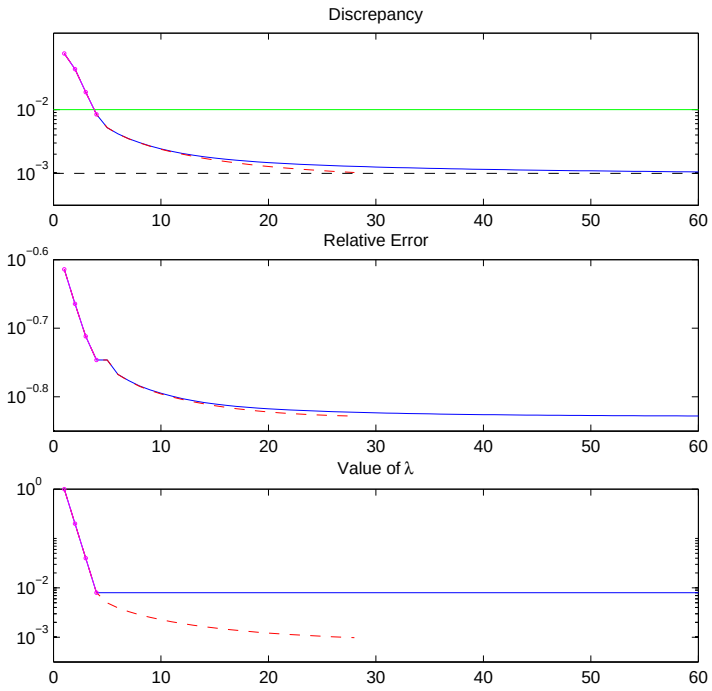


Figure 9: Results of Algorithm 3 applied to the restoration of `mri.tif` with overestimated noise level. In the first box we also plot two horizontal lines, which represent the overestimated and the true noise level. In each box, the initial 4 iterations, corresponding to the first call of Algorithm 2, are highlighted using a small circle. The continuous line represents the slower version of Algorithm 3 (without Step 3), the dashed line represents its quicker version (with Step 3).

In Figure 10 and 11 we compare the quality of the reconstruction after the first call (when the overestimated discrepancy principle is satisfied) and at the end of the scheme using Step 3 of Algorithm 3.

The numerical experiments performed on various kind of discrete ill-posed problems has proved that this approach is really robust and fairly accurate. We have not found examples in which the procedure failed. The method is restarted many times until the discrepancy is almost constant and this constant is much close to the real noise level.

We remark that generally each restart of the method allows to satisfy (27) after the first step of the Arnoldi algorithm, and hence without an heavy extra work. Anyway, since the discrepancy typically stagnates, one may even try to

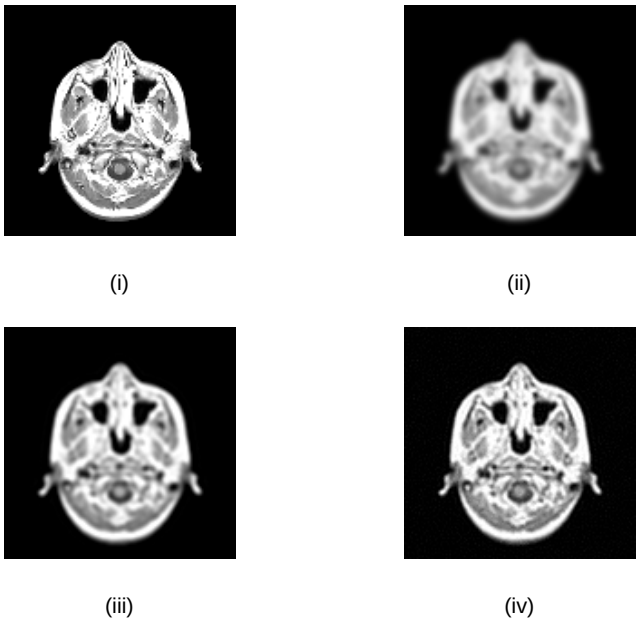


Figure 10: Restoration of `mri.tif`. Original image **(i)**, blurred and noisy image **(ii)**, restoration after the first 4 steps **(iii)**, restoration with Algorithm 3 after 24 restarts **(iv)**.

employ a rational extrapolation to avoid too many restarts, and then apply Algorithm 2 using the extrapolated value.

# 6 Conclusions

In this paper we have proposed an approximated version of the classical discrepancy principle that can be easily coupled with the iterative scheme of the Arnoldi-Tikhonov method, since it simultaneously determines the best value of the regularization parameter $\lambda$ and the dimension $m$ of the reduced problem. This technique is considerably fast and simpler than others commonly used, since it only exploits quantities that are naturally related to the problem we want to solve. The numerical experiments that we have performed so far show that the results computed by our new algorithm are comparable, if not better, to the results computed using the most established methods. Moreover, the robustness and the simplicity of the approach described allows to employ it even as noise-level detector, as demonstrated experimentally in Section 5.

Therefore we strongly believe that the method described in this paper could

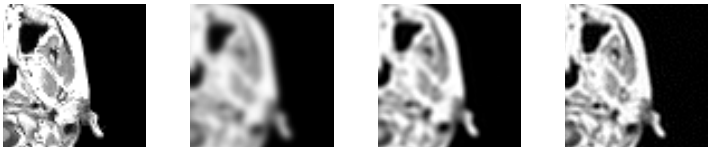


Figure 11: Restoration of `mri.tif`. Blow-up of the corresponding images shown in Figure 10.

be successfully employed to regularize huge ill-posed linear problems coming from many applications, especially the ones concerning the deblurring and denoising of corrupted images.

# References

[1] Å. Björck, *A bidiagonalization algorithm for solving large and sparse ill-posed systems of linear equations*, BIT 28 (1988) 659 670.

[2] D. Calvetti, S. Morigi, L. Reichel, F. Sgallari, *Tikhonov regularization and the L-curve for large discrete ill-posed problems*, J. Comput. Apll. Math. 123 (2000) 423-446.

[3] M. Hanke, P.C. Hansen, *Regularization methods for large-scale problems*, Surv. Math. Ind. 3 (1993) 253-315.

[4] P.C. Hansen, *Regularization Tools: A Matlab package for analysis and solution of discrete ill-posed problems*, Numerical Algorithms, 6 (1994) 1-35.

[5] P.C. Hansen, *Rank-Deficient and Discrete Ill-Posed Problems. Numerical Aspects of Linear Inversion.* SIAM, Philadelphia, 1998.

[6] P.C. Hansen, *Regularization Tools version 3.0 for Matlab 5.2*, Numer. Algorithms, 20 (1999), pp. 195-196.

[7] P.C. Hansen, J.G. Nagy, D.P. O'Leary, *Deblurring Images. Matrices, Spectra and Filtering.* SIAM, Philadelphia, 2006.

[8] M.E. Kilmer, D.P. O'Leary, *Choosing regularization parameters in iterative methods for ill-posed problems*, SIAM J. Matrix Anal. Appl. 22 (2001) 1204 1221.

[9] M.E. Kilmer, P.H. Hansen, M.I. Español, *A projection-based approach to general-form Tikhonov regularization*, SIAM J. Sci. Comput. 29 (2007), no. 1, 315–330

[10] B. Lewis, L. Reichel, *Arnoldi-Tikhonov regularization methods*, J. Comput. Appl. Math 226 (2009) 92-102.

[11] D.P. O'Leary, J.A. Simmons, *A bidiagonalization-regularization procedure for large-scale discretizations of ill-posed problems*, SIAM J. Sci. Statist. Comput. 2 (1981) 474 489.

[12] L. Reichel, A. Shyshkov, *A new zero-finder for Tikhonov regularization*, BIT 48(2008) 627-643.

[13] L. Reichel, Q. Ye, *Simple square smoothing regularization operators*, Electron. Trans. Numer. Anal. 33 (2009) 63-83.

[14] L. Reichel, F. Sgallari, Q.Ye, *Tikhonov regularization based on generalized Krylov subspace methods*, Appl. Numer. Math. (2010), doi:10.1016/j.apnum.2010.10.002 (article in press).

[15] L. Reichel and G. Rodriguez *Old and new parameter choice rules for discrete ill-posed problems*. Submitted, 2012.

[16] Y. Saad *Iterative methods for Sparse Linear Systems*, 2nd edition, SIAM, Philadelphia, 2003.